


RESEARCH ARTICLE

Comparative study of the *Rheum tanguticum*'s chemical contents based on spatial distribution characteristicsYafei Guo¹✉, Qiang Cao¹✉, Mei Guo^{1,2*} , Junmei Wang¹, Renbo Kou¹, Leilei Ye¹**1** College of Pharmacy, Gansu University of Chinese Medicine, Lanzhou, China, **2** Key Laboratory for Chemistry and Quality of Traditional Chinese Medicine & Tibetan Medicine of Gansu Provincial Colleges, Lanzhou, China

✉ These authors contributed equally to this work.

* guomei@gszy.edu.cn OPEN ACCESS**Citation:** Guo Y, Cao Q, Guo M, Wang J, Kou R, Ye L (2022) Comparative study of the *Rheum tanguticum*'s chemical contents based on spatial distribution characteristics. PLoS ONE 17(11): e0278113. <https://doi.org/10.1371/journal.pone.0278113>**Editor:** Clara Sousa, Universidade Católica Portuguesa Escola Superior de Biotecnologia; Universidade Católica Portuguesa Escola Superior de Biotecnologia, PORTUGAL**Received:** March 30, 2022**Accepted:** November 10, 2022**Published:** November 29, 2022**Copyright:** © 2022 Guo et al. This is an open access article distributed under the terms of the [Creative Commons Attribution License](https://creativecommons.org/licenses/by/4.0/), which permits unrestricted use, distribution, and reproduction in any medium, provided the original author and source are credited.**Data Availability Statement:** All relevant data are within the paper.**Funding:** This work was supported by the key Project of Joint Funds of the National Natural Science Foundation of China (U21A20412); the Provincial Natural Science Foundation of Gansu Province, China (21JR7RA558); Excellent doctoral student program of Gansu Province, China (22JR5RA576); the "Double First-Class" key

Abstract

Rheum tanguticum (*R. tanguticum*) has been widely used for the treatment of inflammatory diseases in clinical. However, limited research exist on the quality evaluation of various *R. tanguticum* locations, which has certain drawbacks. In this study, Fourier-transform infrared spectroscopy (FTIR) and high-performance liquid chromatography (HPLC) were used to comparative study on the chemical contents of *R. tanguticum*, to clarify the relationship between the chemical contents and the spatial distribution of *R. tanguticum*. First of all, the FTIR spectra of 18 batches of *R. tanguticum* were examined. Following the cluster analysis, the FTIR spectra of various production locations differed. To some extent, establishing the double index analysis sequence of common and variation peaks may differentiate distinct production locations of medicinal materials. The HPLC fingerprint of *R. tanguticum* was constructed to further explore the link between components and their origin. PCA of common peaks of 18 batches of *R. tanguticum* indicated that *R. tanguticum* grown in Gannan and Qinghai had a tendency to separate [2], however this trend was not noticeable. Then, OPLS-DA model was established, and the key differential components of *R. tanguticum* produced in Gannan and Qinghai were discovered to be R16, R37, R46, and R47 (Aloe emodin) ($VIP \geq 1$ and $P < 0.05$). At last, Pearson's test was used to examine the relationship between longitude, latitude, altitude, and composition. Longitude was significantly positively correlated with R28 and R30 ($P < 0.05$), and a very significantly positively correlated with R35, R36, R37, R46, and R47 ($P < 0.01$). Latitude was significantly negatively correlated with R34, R35, and R40 ($P < 0.05$), and extremely significantly negatively correlated with R28, R30, R36, R37, R46, and R47 ($P < 0.01$). Altitude was significantly positive correlation with R36 and R37 ($P < 0.01$). The results of our study can provide insights into *R. tanguticum* quality control and aid in establishing a natural medication traceability system.

Introduction

Rhubarb is a traditional Chinese medicine and the most widely used natural medication globally, with primary sources being dried roots and rhizomes. *Rheum tanguticum* (*R. tanguticum*)

Scientific Research Project of the Department of Education of Gansu Province, China (GSSYLXM-05); The Project of Central Government Guides the Development of Local Science and Technology, Gansu Province, China. The funders had no role in study design, data collection and analysis, decision to publish, or preparation of the manuscript.

Competing interests: The authors have declared that no competing interests exist.

is one of the main sources of rhubarb. *Rheum tanguticum* Maxim is a Polygonaceae ex Balf plant, which is mostly grown in southern Gansu and southern Qinghai provinces [1]. The primary active constituents of rhubarb are anthraquinone, double anthrone, and tannin. Its primary pharmacological effects include inducing constipation and anti-inflammatory, diuretic, antibacterial, and antitumor properties [2–4]. Anti-inflammatory is one of the most important pharmacological effects of rhubarb. Rhubarb has been also used to treat inflammation-related diseases in clinical, such as acute pancreatitis, acute cholecystitis, appendicitis, ulcerative colitis and so on [5–9]. The administration of rhubarb extract reduced the expression of key inflammatory genes (TLR4, MCP-1, TNF- α , IL-6), macrophage-related markers (F4/80, CD68, CD11c) and oxidative markers (TLR4, NADPH oxidase). Rhubarb can eliminate inflammatory mediators from tissue and plasma and drastically reduce tumor necrosis factor (TNF), interleukin, and endotoxin levels in the serum of patients suffering from or successfully treated with severe pancreatitis by blocking the production of the inflammatory factor HMGB-1 [10]. Rhubarb aqueous extract not only inhibit the inflammatory response induced by TNF- α and the augmentation or rise of adhesion molecules in human umbilical vein endothelial cells (HUVECs), but also reduce adhesion between U937 cells and HUVECs [11]. The rhubarb extract modified host antimicrobial peptide production and gut homeostasis and was associated with profound changes in gut microbial composition [12,13]. Previous studies showed that rhubarb components, such as emodin, rhein, chrysophanol, lindleyin, and isolotus anthocyanins, have anti-inflammatory properties [11,14,15]. Emodin inhibits lipopolysaccharide (LPS)-induced apoptosis and inflammation by increasing the expression of the TUG1 (Long non-coding RNA) in cartilage-derived ATDC5 cells [16]. Emodin and Rhein exhibit potent anti-inflammatory actions in LPS-induced Raw 264.7 cells [17,18]. Chrysophanol may ameliorate LPS-induced inflammation in mice, minimize pathological harm to the liver and lung tissues, and lower blood TNF- α levels [19]. Derived from rhubarb, lindleyin and isolotus palmoside have anti-inflammatory and analgesic properties [20]. For the study of the anti-inflammatory mechanism of rhubarb, most of them focus on the study of components (such as: emodin, rhein) [21,22]. Several studies showed that the inflammatory effect of emodin was involved in the inactivation of NF- κ B, an essential regulator of inflammatory processes, and PPAR γ -dependent pathway was possibly involved in the NF- κ B inhibitive effect of emodin [23,24]. Rhein significantly decreased IL-1 β secretion via NLRP3 inflammasomes by disturbing their assembly in macrophages. Rhein also activated the Nrf2-HO1-NQO1 pathway and inhibited expression of Nox2 subunits and translocation to regulate redox balance. Moreover, rhein attenuated inflammatory responses by mediating macrophage polarization from M1 to M2 phenotype. NF- κ B, AP-1, and MAPK signalling were also involved in improving inflammatory conditions by rhein [25–27]. With the development and progress of natural medication, quality control has been the most crucial factor in current research [20]. The quality of rhubarb in the market is variable because of mixed varieties, varying processing processes, and manufacturing locales [28]. Numerous studies have been conducted on the quality control of rhubarb to maximize the impact of natural medications; however, those on the variations in *R. tanguticum* from different production locations are limited [29–31]. This is not conducive to the clinical application of *R. tanguticum* from different origins.

To better manage the internal quality of natural drugs, modern analytical methods, such as spectroscopy and chromatography, have been widely utilized in quality control to compensate for the weakness of conventional morphological and anatomical identification of the source of natural pharmaceuticals. These sophisticated analytical approaches not only objectively represent internal quality, but also compensate for the lack of personal expertise. Some authors have recently described plant drug control analytical approaches, such as chromatography, spectrum, DNA barcoding, and other analytical methods [32–35]. Spectral and chromatographic

approaches are mostly utilized in categorizing and identifying original plants as well as in evaluating quality and identifying the origin. These two approaches can explain some additional chemical information simultaneously, and the resulting fingerprint has become an established method for evaluating quality consistency. Fourier-transform infrared spectroscopy (FTIR) and high-performance liquid chromatography (HPLC) are two such techniques. FTIR has been widely used to determine the provenance of food and natural pharmaceuticals as well as to forecast the quantity of index components [36,37]. Many agencies, including the World Health Organization, Food and Drug Administration, and State Food and Drug Administration, have acknowledged HPLC fingerprint [38]. These two approaches, in conjunction with chemometrics, have been effectively used for the quality control and origin identification of a wide range of natural pharmaceuticals. Simple and quick measurement methods bypass the time-consuming pretreatment procedure for quality analysis and do not require a significant number of chemical reagents.

In this study, the FTIR spectra of 18 batches of *R. tanguticum* were examined by FTIR. Cluster analysis and the double index sequence method were used for distinguish *R. tanguticum* regions. The HPLC fingerprint of *R. tanguticum* was constructed by HPLC. And PCA, OPLS-DA was used for study the differential components of *R. tanguticum* in Gannan and Qinghai. At last, pearson correlation test was used for preliminarily clarified the relationship between chemical contents of *R. tanguticum* and longitude, latitude, altitude. The results of this study could encourage the growth of *R. tanguticum* business and to assist in implementing a natural medication traceability system.

Materials and methods

Herbal medicine

Yuwei Gan, Agricultural Technology Extension Researcher at the Gannan Science and Technology Development and Exchange Center, confirmed the authenticity of the *R. tanguticum* sample. For more information, refer to [Table 1](#).

FTIR study

Instrument parameter setting. A Nicolet 6700 FT-IR spectrometer (Thermo Fisher, America) with a silicon carbide rod light source, DTGs detector, 4 cm^{-1} resolution, 30 scanning accumulation, detection in the spectral range of $4000\text{--}400\text{ cm}^{-1}$, room temperature, and the interference of H_2O and CO_2 was deducted.

Sample preparation. *R. tanguticum* was crushed and sieved through a 100 mesh sieve (Huafeng Hardware Instrument Co., Ltd., Shaoxing, China). Ultrasonic extraction of 1.00 g of powder with 50 mL methanol (AR, Lot No.: 20200825, Tianjin Fuyu Fine Chemical Co., Ltd., Tianjin, China) was performed for 1 h (20 kHz, $30\pm 5\text{ }^\circ\text{C}$). Then, suction filtration was performed and the methanol was evaporated to obtain the *R. tanguticum* methanol extract, which was labeled M1–M18.

Approximately 1 mg of *R. tanguticum* methanol-extracted powder was mixed with 100 mg of KBr (for IR, Lot No.: 20200715, Damao Chemical Reagent Factory, Tianjin, China) and compressed into a tablet. KBr was used as a blank, and infrared spectrum data for both samples were collected.

Infrared spectrum data analysis. The OMNIC 8.2 software and Origin software (version 9.0) were used for automated baseline correction, smoothing, and ordinate normalization of infrared spectrum findings.

Table 1. Rheum tanguticum sample information.

label	Collecting Time	Source	Longitude/°E	Latitude/°N	Altitude/m
1	Autumn, 2017	Hezuo	102.91	35.00	3136
2	Spring, 2019	Hezuo	102.91	35.00	3136
3	Autumn, 2019	Hezuo	102.91	35.00	3136
4	Autumn, 2018	Hezuo	102.91	35.00	3136
5	Autumn, 2018	Hezuo	102.91	35.00	3136
6	Autumn, 2018	Hezuo	102.91	35.00	3136
7	Autumn, 2018	Hezuo	102.91	35.00	3136
8	Autumn, 2017	Hezuo	102.91	35.00	3136
9	Autumn, 2019	Xiahe, Hezuo	102.52	35.20	3471
10	Autumn, 2019	Lintan, Hezuo	103.35	34.69	2867
11	Autumn, 2019	Qinghai	101.77	36.65	2261
12	Autumn, 2019	Qinghai	101.77	36.65	2261
13	Autumn, 2018	Qinghai	101.77	36.65	2261
14	Autumn, 2018	Qinghai	101.77	36.65	2261
15	Autumn, 2019	Huangzhong, Qinghai	101.57	36.50	2600
16	Autumn, 2018	Huangzhong, Qinghai	101.57	36.50	2600
17	Autumn, 2018	Datong, Qinghai	101.69	36.93	3451
18	Autumn, 2017	Guide, Qinghai	101.44	36.07	2200

<https://doi.org/10.1371/journal.pone.0278113.t001>

Double index sequence analysis of common peak rate and variation peak rate

$$P = \frac{N_g}{N} \times 100\% \quad (1)$$

$$P_a = \frac{N_a}{N_g} \times 100\% \quad (2)$$

$$P_b = \frac{N_b}{N_g} \times 100\% \quad (3)$$

Note: P is the common peak rate of the two samples; N is the number of independent peaks in the two samples; N_g is the common peak number of the two samples; P_a is the variation peak rate of the sample; N_a is the variation peak rate of the sample; P_b is the variation peak rate of sample B; N_b is the variation peak number of sample B, which conforms to $N = N_g + N_a + N_b$.

The common peak rate and variation peak rate of the infrared spectrum between M1 and M18 were determined using (1)–(3), and the Rhubarb double index analysis sequence was created. The sequence has great identification ability and can accurately estimate the genetic distance between all samples in the 2+n-dimensional ($n = \text{number of samples}$) space [39]. M_a : M_b (P; P_a , P_b) is the double index analysis sequence of the common peak rate and variation peak rate, which implies that with M_a as the control medication, the common peak rate of M_b is P, the variation peak rate of M_a is P_a , and the variation peak rate of M_b is P_b .

HPLC study

Chromatographic conditions. The Agilent 1260 High performance liquid chromatography (Agilent Technologies, USA), with an Agilent TC-C18(2) chromatographic column

(4.6×250 mm, 5 μm) was utilized. The flow rate was 1 mL·min⁻¹, column temperature was 30 °C, detection wavelength was 280 nm, and injection volume was 5 μL. The mobile phase comprised methanol (A) and 0.1% formic acid in water (B). The gradient elution procedure was: 0–6 min, 10%–30% A; 6–13 min, 30%–33% A; 13–21 min, 33%–37% A; 21–25 min, 37%–40% A; 25–35 min, 40%–45% A; 35–45 min, 45%–48% A; 45–49 min, 48%–52% A; 49–54 min, 52%–60% A; 54–64 min, 60%–95% A; 64–74 min, 95%–10% A; 74–78 min, 10% A.

Sample preparation. Ultrasonic extraction was performed on 1.00 g rhubarb powder and 50 mL methanol for 1 h (20 kHz, 30±5 °C). The sample was filtered using 0.45 μm microporous membrane filtration. The filtered sample was marked as S1–S18.

The single standard and mixed standard solutions were prepared with methanol at a concentration of 1 mg/mL for each pharmacopoeia standard (purity ≥ 98%) of emodin (Lot No. 1205A0210), rhein (Lot No. 109C021), chrysophanol (Lot No. 523D025), aloë emodin (Lot No. 531B024), emodin methyl ether (Lot No. 718C023), catechin (Lot No. 1125H021), gallic acid (Lot No. 725G028), and sennoside A (Lot No. AF9111318) and sennoside B (Lot No. AF9111319).

Establish fingerprint. The S1–S18 chromatographic data was imported into the "Similarity evaluation system for chromatographic fingerprint of TCM (Version 2012)," for which the *R. tanguticum* fingerprint was created. Then, the similarity of S1–S18 was analyzed.

Analysis of chemometrics methods. The spectrum of S1–S18 chromatographic data was imported into the SIMCA software. The missing value was replaced with half of the minimum value, and the component was eliminated if the missing value reached 20%. The HPLC data matrix was statistically analyzed using PCA. The data were separated into two groups based on their origin, and OPLS-DA was performed to compare the groups.

Results and analysis

The results from the FTIR study

Similarity analysis results. The FTIR spectra of M1–M18 are shown in Fig 1 and exhibit certain similarities. Absorption peaks were observed at 400–1800 cm⁻¹ and 2700–3800 cm⁻¹.

The spectra were analyzed for similarity; the results are presented in Table 2. The similarity of the FTIR spectra ranged from 0.863 to 0.988, with a high overall similarity, demonstrating that the composition and content of *R. tanguticum* were relatively stable. Regarding sample similarity analysis, in M1–M10, 97.78 percent were greater than 0.9 and 96.43% of the samples in M11–M18 had similarity greater than 0.9. The similarity between M1–M10 and M11–M18 was greater than 0.9, accounting for 92.50%, demonstrating a high similarity between the M1–M10 and M11–M18 groups. The similarity between M1–M10 and M11–M18 was slightly lower.

The similarity of rhubarb methanol extract from the same origin was significant, whereas that of rhubarb from other sources was somewhat different. The rhubarb-producing locations can be differentiated using infrared chromatography.

Confirmation of common peaks and peak attribution. If the greatest difference in the wave number of a group of absorption peaks was smaller than the difference in the average wave number of its surrounding groups of peaks, the group of peaks was defined as a group of common peaks.

According to the absorption peak data reported by the OMNIC software, 17 peaks were found in the alcohol extract using standard peak identification methods. The wavenumber and common FTIR absorption peaks were listed (Table 3). Common peaks in the distinctive region were assigned as Table 4.

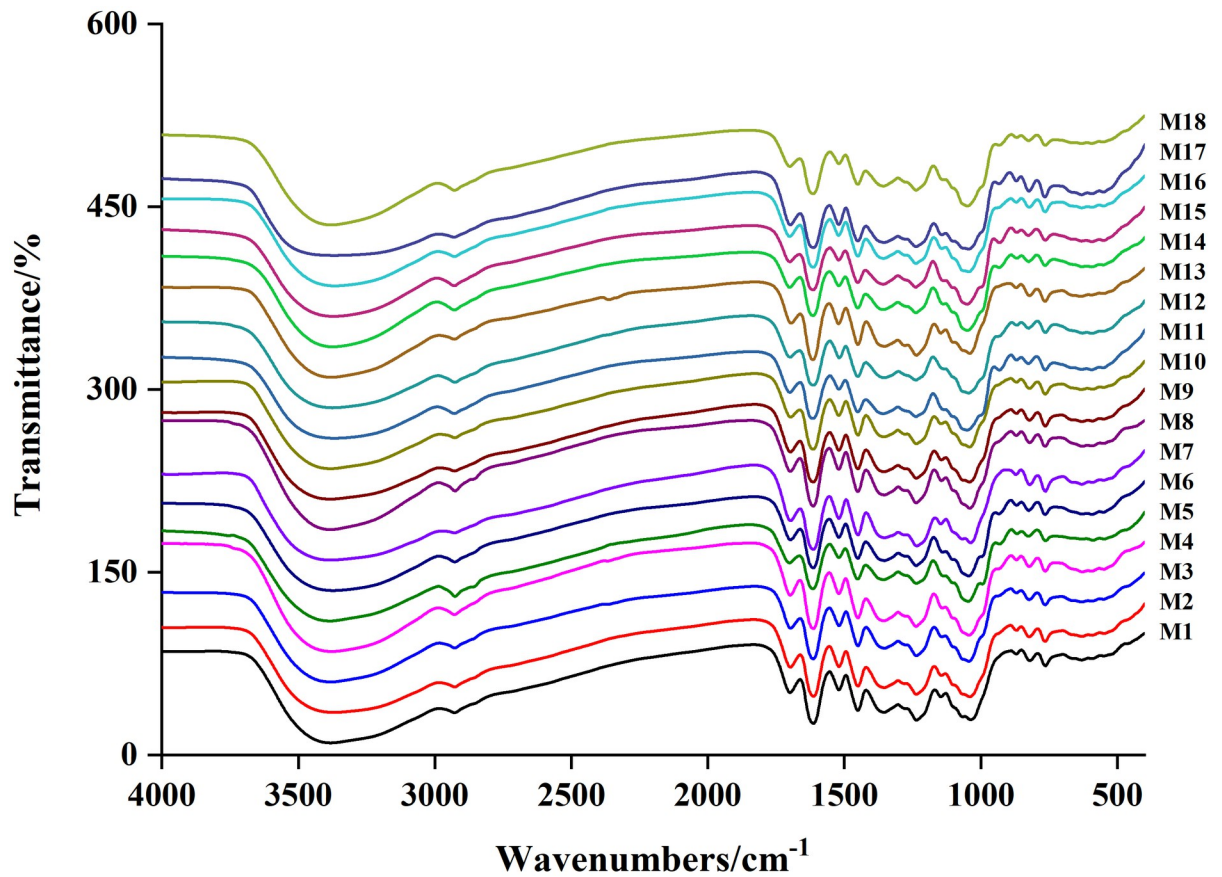


Fig 1. The FTIR spectra of M1 ~ M18.

<https://doi.org/10.1371/journal.pone.0278113.g001>

Table 2. Similarity analysis of FTIR spectrum of M1~M18.

Sample	M1	M2	M3	M4	M5	M6	M7	M8	M9	M10	M11	M12	M13	M14	M15	M16	M17	M18
M1	1.000																	
M2	0.929	1.000																
M3	0.969	0.967	1.000															
M4	0.977	0.930	0.957	1.000														
M5	0.991	0.927	0.968	0.981	1.000													
M6	0.919	0.938	0.966	0.893	0.915	1.000												
M7	0.972	0.950	0.972	0.960	0.969	0.918	1.000											
M8	0.976	0.956	0.969	0.988	0.979	0.907	0.973	1.000										
M9	0.945	0.950	0.982	0.922	0.940	0.970	0.954	0.936	1.000									
M10	0.951	0.974	0.989	0.932	0.945	0.974	0.963	0.950	0.985	1.000								
M11	0.954	0.948	0.981	0.923	0.948	0.975	0.953	0.933	0.982	0.982	1.000							
M12	0.892	0.955	0.959	0.863	0.884	0.973	0.917	0.890	0.974	0.981	0.969	1.000						
M13	0.970	0.971	0.982	0.966	0.971	0.946	0.974	0.977	0.966	0.974	0.972	0.936	1.000					
M14	0.967	0.913	0.944	0.961	0.960	0.890	0.951	0.962	0.924	0.929	0.930	0.867	0.964	1.000				
M15	0.970	0.968	0.987	0.951	0.969	0.959	0.975	0.964	0.974	0.983	0.983	0.954	0.989	0.947	1.000			
M16	0.963	0.962	0.985	0.944	0.957	0.975	0.961	0.954	0.983	0.987	0.984	0.965	0.982	0.947	0.985	1.000		
M17	0.941	0.973	0.983	0.920	0.936	0.975	0.957	0.940	0.982	0.992	0.984	0.983	0.972	0.920	0.984	0.985	1.000	
M18	0.927	0.942	0.965	0.887	0.915	0.966	0.933	0.906	0.969	0.977	0.973	0.974	0.940	0.892	0.964	0.969	0.982	1.000

<https://doi.org/10.1371/journal.pone.0278113.t002>

Table 3. Common peaks of M1~M18 FTIR absorption.

Sample	Wave number/cm ⁻¹								
	M1	3380.70	2927.14	1697.90	1609.27	1513.93	1449.18	1354.62	1238.54
M2	3369.65	2929.21	1697.46	1609.02	1514.56	1448.76	1355.84	1237.49	1142.48
M3	3365.17	2927.10	1698.14	1609.14	1516.28	1448.93	1355.10	1238.36	1142.77
M4	3372.86	2928.06	1697.77	1609.98	1513.94	1449.07	1358.24	1238.85	—
M5	3373.23	2927.81	1700.74	1610.45	1514.33	1449.34	1354.00	1239.39	—
M6	3377.44	2928.13	1696.30	1611.60	1518.16	1448.93	1356.21	1236.71	1143.82
M7	3373.34	2925.65	1698.39	1608.92	1513.96	1448.88	1355.33	1239.76	—
M8	3369.39	2928.44	1697.80	1609.48	1513.64	1449.08	1357.40	1238.86	—
M9	3381.26	2926.57	1696.72	1609.89	1514.66	1448.86	1353.83	1237.44	1142.66
M10	3384.23	2926.82	1697.2	1609.02	1514.14	1448.9	1355.01	1237.69	1142.93
M11	3383.08	2924.68	1697.66	1610.43	1515.44	1448.74	1352.77	1238.20	1142.69
M12	3380.62	—	1696.67	1609.32	1513.83	1448.65	1353.16	1235.59	1143.66
M13	3372.38	2927.02	1697.51	1610.12	1514.12	1449.00	1355.88	1237.88	1141.40
M14	3385.58	2925.70	1701.26	1610.35	1514.26	1449.86	1359.77	1238.85	—
M15	3374.93	2927.39	1698.17	1609.31	1514	1448.81	1359.02	1238.53	1141.64
M16	3377.28	2926.61	1697.03	1611.27	1512.78	1448.79	1354.26	1236.87	1142.65
M17	3376.22	2926.82	1697.52	1609.02	1513.33	1448.57	1355.31	1237.06	1143.23
M18	3381.82	2926.51	1697.71	1609.27	1513.68	1448.78	1356.17	1236.50	1143.94
Average	3376.62	2927.04	1697.89	1609.77	1514.39	1448.95	1355.66	1237.92	1142.82
Maximum difference	20.41	4.53	4.96	2.68	5.38	1.29	7.00	4.17	2.54

Sample	Wave number/cm ⁻¹								
	M1	1048.35	—	869.52	825.15	766.81	629.04	—	—
M2	1044.86	944.03	869.54	823.00	767.14	627.93	—	547.63	—
M3	1044.46	—	869.47	818.49	766.67	630.74	—	—	—
M4	1048.82	926.47	870.92	822.44	767.20	—	594.23	—	—
M5	1048.76	—	870.64	819.03	767.21	—	598.34	—	—
M6	1038.13	—	868.09	821.76	767.35	634.63	—	—	—
M7	1045.11	—	869.04	826.91	766.31	—	590.36	—	—
M8	1049.24	926.40	868.71	826.88	767.18	—	593.47	—	—
M9	1037.93	—	871.05	818.49	766.24	630.89	—	—	—
M10	1038.07	—	869.30	818.37	766.74	628.60	—	—	—
M11	1038.08	—	869.10	819.10	766.84	627.45	—	—	—
M12	1035.60	—	870.04	818.61	766.29	629.53	—	—	—
M13	1044.86	—	868.77	825.29	766.59	—	596.19	—	—
M14	1045.96	—	867.50	826.28	765.96	—	584.16	—	—
M15	1041.91	—	869.19	817.62	766.28	628.76	—	547.37	—
M16	1040.83	—	868.43	822.38	766.47	625.63	—	—	—
M17	1038.24	—	869.64	818.32	766.45	629.04	—	—	—
M18	1035.73	—	869.48	817.30	765.36	628.65	—	—	—
Average	1042.50	932.30	869.36	821.41	766.67	629.24	592.79	547.50	—
Maximum difference	13.64	17.63	3.55	9.61	1.99	9.00	14.18	0.26	—

"—" means that the sample has no this wave number.

<https://doi.org/10.1371/journal.pone.0278113.t003>

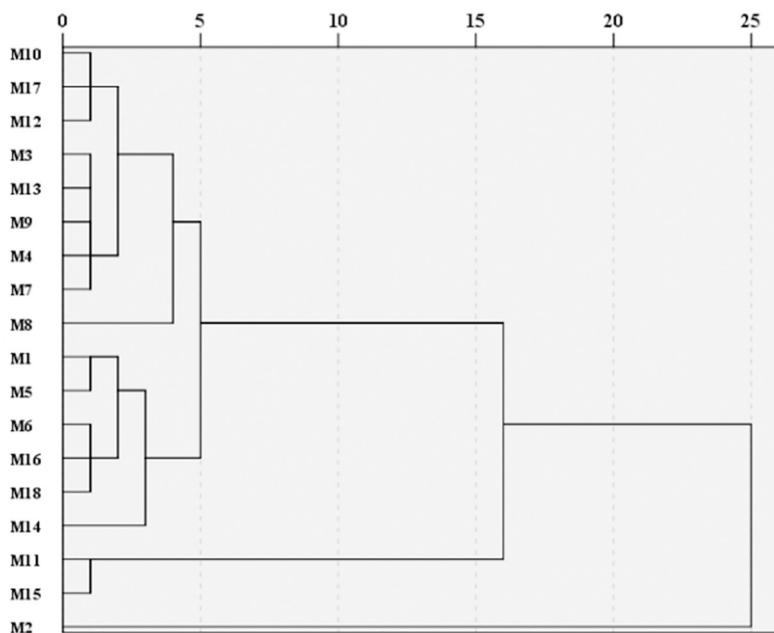
Table 4. Vibrational modes of functional groups in common peaks (distinctive region).

Wave number/ cm ⁻¹	Peak intensity	Vibration mode
3415.27– 3359.21	wide and strong peak	polymer ν (O-H), amide ν (N-H)
2932.79– 2924.68	acromion	methylene ν (C-H)
1701.26– 1696.30	moderately strong peak	ν (C = O)
1626.70– 1608.92	medium strong peak	amide β (N-H)
1520.35– 1512.78	weak peak	amide β (N-H), aromatic hydrocarbon, and benzene ring skeleton vibration ν (C = C)
1449.86– 1446.70	medium strong peak	methyl δ (C-H), methylene δ (C-H), β (O-H), aromatic hydrocarbon, and benzene ring skeleton vibration ν (C = C)
1367.46– 1316.93	medium strong peak	methyl β (C-H)
1243.07– 1235.59	moderately strong peak	δ (O-H), ν (C-N), and ν (C-O-C)
1146.30– 1141.00	medium strong peak	ν (C-N) of lipid compounds ν (C-O-C)
1053.72– 1033.93	strong peak	δ (C-O)

<https://doi.org/10.1371/journal.pone.0278113.t004>

R. tanguticum was mostly composed of anthraquinones, polysaccharides, and tannins. The FTIR analysis results were consistent with the composition research findings, and the methanol extract included the majority of the *R. tanguticum* components.

Cluster analysis. SPSS 26 software was used to perform systematic cluster analysis of M1–M18. The interval was the square Euclidean distance, and the cluster technique was the

**Fig 2. FTIR cluster analysis diagram of M1 ~ M18.**

<https://doi.org/10.1371/journal.pone.0278113.g002>

Table 5. The sequence with the same absorption peak (Group A).

Control Sample	Comparison Sample	(P; Pa, Pb)	Control Sample	Comparison Sample	(P; Pa, Pb)
M3	M6M9M10M11M16M17M18	(1.0000; 0.0000, 0.0000)	M4	M8	(1.0000; 0.0000, 0.0000)
M5	M7M14	(1.0000; 0.0000, 0.0000)	M6	M3M9M10M11M16M17M18	(1.0000; 0.0000, 0.0000)
M7	M5M14	(1.0000; 0.0000, 0.0000)	M8	M4	(1.0000; 0.0000, 0.0000)
M9	M3M6M10M11M16M17M18	(1.0000; 0.0000, 0.0000)	M10	M3M6M9M11M16M17M18	(1.0000; 0.0000, 0.0000)
M11	M3M6M9M10M16M17M18	(1.0000; 0.0000, 0.0000)	M14	M5M7	(1.0000; 0.0000, 0.0000)
M16	M3M6M9M10M11M17M18	(1.0000; 0.0000, 0.0000)	M17	M3M6M9M10M11M16M18	(1.0000; 0.0000, 0.0000)
M18	M3M6M9M10M11M16M17	(1.0000; 0.0000, 0.0000)			

<https://doi.org/10.1371/journal.pone.0278113.t005>

intergroup connection method. Cluster analysis was performed on 18 batches of FTIR spectra (Fig 2). When the Euclidean Distance was 10, it was separated into three groups: M10M17M12M3M13M9M4M7M8M1M5M6M16M18M14, M11M15, and M2. This might be owing to the cumulative impact of geographical location, soil, and weather. The chemical content of rhubarb varied depending on the location of its growth.

The results of the double index sequence analysis. Basic grouping was employed in the M1–M18 sequence. According to the common peak rate, the most comparable sample pairs and groups could be sorted into the Tables 5–8.

Table 6. The sequence with high common peak rate and low variation peak rate (Group B).

Control Sample	Comparison Sample	(P; Pa, Pb)	Control Sample	Comparison Sample	(P; Pa, Pb)
M1	M3M6M9M10M11M16M17M18	(0.9286; 0.0000, 0.0769)	M1	M5M7M12M14	(0.8571; 0.0833, 0.0833)
M2	M15	(0.9375; 0.0667, 0.0000)	M2	M1M12M13	(0.8125; 0.2308, 0.0000)
M3	M15	(0.9333; 0.0000, 0.0714)	M3	M1M12	(0.9286; 0.0769, 0.0000)
M3	M13	(0.8667; 0.0769, 0.0769)	M4	M5M7M14	(0.9286; 0.0769, 0.0000)
M4	M13	(0.8125; 0.0769, 0.0769)	M5	M4M8M13	(0.9286; 0.0000, 0.0769)
M5	M1	(0.8571; 0.0833, 0.0833)	M6	M15	(0.9333; 0.0000, 0.0714)
M6	M1M12	(0.9286; 0.0769, 0.0000)	M6	M13	(0.8667; 0.0769, 0.0769)
M7	M4M8M13	(0.9286; 0.0000, 0.0769)	M7	M1	(0.8571; 0.0833, 0.0833)
M8	M5M7M14	(0.9286; 0.0769, 0.0000)	M8	M13	(0.8667; 0.0769, 0.0769)
M9	M15	(0.9333; 0.0000, 0.0714)	M9	M1M12	(0.9286; 0.0769, 0.0000)
M9	M13	(0.8667; 0.0769, 0.0769)	M10	M15	(0.9333; 0.0000, 0.0714)
M10	M1M12	(0.9286; 0.0769, 0.0000)	M10	M13	(0.8667; 0.0769, 0.0769)
M11	M15	(0.9333; 0.0000, 0.0714)	M11	M1M12	(0.9286; 0.0769, 0.0000)
M11	M13	(0.8667; 0.0769, 0.0769)	M12	M3M6M9M10 M11M16M17M18	(0.9286; 0.0000, 0.0769)
M12	M1	(0.8571; 0.0833, 0.0833)	M13	M5M7M14	(0.9286; 0.0769, 0.0000)
M13	M3M6M8M9M10 M11M16M17M18	(0.8667; 0.0769, 0.0769)	M13	M4	(0.8125; 0.0769, 0.0769)
M14	M4M8M13	(0.9286; 0.0000, 0.0769)	M14	M1	(0.8571; 0.0833, 0.0833)
M15	M2	(0.9375; 0.0000, 0.0667)	M15	M3M6M9M10 M11M16M17M18	(0.9333; 0.0714, 0.0000)
M16	M15	(0.9333; 0.0000, 0.0714)	M16	M1M12	(0.9286; 0.0769, 0.0000)
M16	M13	(0.8667; 0.0769, 0.0769)	M17	M15	(0.9333; 0.0000, 0.0714)
M17	M1M12	(0.9286; 0.0769, 0.0000)	M17	M13	(0.8667; 0.0769, 0.0769)
M18	M15	(0.9333; 0.0000, 0.0714)	M18	M1M12	(0.9286; 0.0769, 0.0000)
M18	M13	(0.8667; 0.0769, 0.0769)			

<https://doi.org/10.1371/journal.pone.0278113.t006>

Table 7. The sequence with high common peak rate and high variation peak rate (Group C).

Control Sample	Comparison Sample	(P; Pa, Pb)	Control Sample	Comparison Sample	(P; Pa, Pb)
M1	M15	(0.8667; 0.0000, 0.1538)	M1	M2	(0.8125; 0.000, 0.2308)
M1	M4M8M13	(0.8000; 0.0833, 0.1667)	M2	M3M6M9M10 M11M16M17M18	(0.8750; 0.1429, 0.0000)
M3	M2	(0.8750; 0.0000, 0.1429)	M3	M5M7M14	(0.8000; 0.1667, 0.0833)
M4	M1	(0.8000; 0.1667, 0.0833)	M5	M3M6M9M10 M11M16M17M18	(0.8000; 0.0833, 0.1667)
M6	M2	(0.8750; 0.0000, 0.1429)	M6	M5M7M14	(0.8000; 0.1667, 0.0833)
M7	M3M6M9M10M11M16M17M18	(0.8000; 0.0833, 0.1667)	M8	M1	(0.8000; 0.1667, 0.0833)
M9	M2	(0.8750; 0.0000, 0.1429)	M9	M5M7M14	(0.8000; 0.1667, 0.0833)
M10	M2	(0.8750; 0.0000, 0.1429)	M10	M5M7M14	(0.8000; 0.1667, 0.0833)
M11	M2	(0.8750; 0.0000, 0.1429)	M11	M5M7M14	(0.8000; 0.1667, 0.0833)
M12	M15	(0.8667; 0.0000, 0.1538)	M12	M2	(0.8125; 0.0000, 0.2308)
M12	M13	(0.8000; 0.0833, 0.1667)	M13	M15	(0.8125; 0.0769, 0.1538)
M13	M2	(0.8125; 0.0000, 0.2308)	M13	M1M12	(0.8000; 0.1667, 0.0833)
M14	M3M6M9M10M11M16M17M18	(0.8000; 0.0833, 0.1667)	M15	M1M12	(0.8667; 0.1538, 0.0000)
M15	M13	(0.8125; 0.1538, 0.0769)	M16	M2	(0.8750; 0.0000, 0.1429)
M16	M5M7M14	(0.8000; 0.1667, 0.0833)	M17	M2	(0.8750; 0.0000, 0.1429)
M17	M5M7M14	(0.8000; 0.1667, 0.0833)	M18	M2	(0.8750; 0.0000, 0.1429)
M18	M5M7M14	(0.8000; 0.1667, 0.0833)			

<https://doi.org/10.1371/journal.pone.0278113.t007>

The common peak rate and variation peak rate of the sequence were the same in group A, and the absorption peak corresponded completely. The sequence common peak rate was high in group B, whereas its variation peak rate was low. The sequence common peak rate and variation peak rate were higher in Group C. The common peak rate of the sequence was lower in Group D, whereas its variation peak rate was higher.

Table 8. The sequence with low common peak rate and high variation peak rate (Group D).

Control Sample	Comparison Sample	(P; Pa, Pb)	Control Sample	Comparison Sample	(P; Pa, Pb)
M2	M4M8	(0.7674; 0.2308, 0.0769)	M2	M5M7M14	(0.7059; 0.3333, 0.0833)
M3	M4M8	(0.7500; 0.1667, 0.1667)	M4	M2	(0.7674; 0.0769, 0.2308)
M4	M3M6M9M10M11M16M17M18	(0.7500; 0.1667, 0.1667)	M4	M15	(0.7059; 0.1667, 0.1667)
M4	M12	(0.6875; 0.2727, 0.0909)	M5	M15	(0.7500; 0.0833, 0.2500)
M5	M12	(0.7333; 0.1818, 0.1818)	M5	M2	(0.7059; 0.0833, 0.3333)
M5	M2	(0.7059; 0.0833, 0.3333)	M6	M4M8	(0.7500; 0.1667, 0.1667)
M7	M15	(0.7500; 0.0833, 0.2500)	M7	M12	(0.7333; 0.1818, 0.1818)
M7	M2	(0.7059; 0.0833, 0.3333)	M8	M2	(0.7674; 0.0769, 0.2308)
M8	M3M6M9M10M11M16M17M18	(0.7500; 0.1667, 0.1667)	M8	M15	(0.7059; 0.1667, 0.2500)
M8	M12	(0.6875; 0.2727, 0.1818)	M9	M4M8	(0.7500; 0.1667, 0.1667)
M10	M4M8	(0.7500; 0.1667, 0.1667)	M11	M4M8	(0.7500; 0.1667, 0.1667)
M12	M5M7	(0.7333; 0.1818, 0.1818)	M12	M8	(0.6875; 0.1818, 0.2727)
M12	M14	(0.6875; 0.1818, 0.1818)	M12	M4	(0.6875; 0.0909, 0.2727)
M14	M15	(0.7500; 0.0833, 0.2500)	M14	M2	(0.7059; 0.0833, 0.3333)
M14	M12	(0.6875; 0.1818, 0.1818)	M15	M5M7	(0.7500; 0.2500, 0.0833)
M15	M14	(0.7500; 0.2500, 0.0833)	M15	M8	(0.7059; 0.2500, 0.1667)
M15	M4	(0.7059; 0.1667, 0.1667)	M16	M4M8	(0.7500; 0.1667, 0.1667)
M17	M4M8	(0.7500; 0.1667, 0.1667)	M18	M4M8	(0.7500; 0.1667, 0.1667)

<https://doi.org/10.1371/journal.pone.0278113.t008>

Double index analysis and sequence analysis of the methanol extract of rhubarb revealed that different results of *R. tanguticum* from different producing areas. However, the methanol extract can eliminate some differences caused by environmental factors. For example, Hezuo, Hezuo, Xiahe of Hezuo, Lintan of Hezuo, Qinghai, Huangzhong of Qinghai, Datong of Qinghai, and Guide of Qinghai are the corresponding producing areas of sequence M3: M6M9M10M11M16M17M18. Nonetheless, the sequence resulting from double index analysis showed that the common peak rate was 100%, with no variation peak. If this method was used, then the samples were classified into one category.

According to the results of the above analysis, environmental factors such as origin, altitude, longitude, latitude, and climatic conditions could affect the common peak rate and variation peak rate of *R. tanguticum*, but the specific impact could be determined. The components of *R. tanguticum* were determined using HPLC, and the effects of altitude, longitude, and latitude on these components were studied to further analyze the influence of the environment on the quality of *R. tanguticum*.

The result of HPLC study

Chromatography of pharmacopoeia standards. The chromatographic peaks of the mixed pharmacopoeia standards are shown in Fig 3. The chromatographic peaks of the nine components were identified using the chromatographic peak of a single pharmacopoeia standard.

Establish rhubarb fingerprint. HPLC was used to acquire chromatograms of S1–S18 (Fig 4). The S1–S18 spectra were imported into the "Similarity evaluation system for chromatographic fingerprint of TCM (version 2012)" and S1 was set as the control spectrum for chromatographic peak matching to obtain the *R. tanguticum* common peak pattern spectrum (Fig 5). A total of 53 peaks were observed. Eight chromatographic peaks were identified after the retention time and compared with the chromatogram of the reference material.

The fingerprints of the 18 batches of Rheum tanguticum were nearly identical. The similarity of each batch to the standard fingerprint was 0.909, 0.861, 0.888, 0.895, 0.879, 0.620, 0.671, 0.899, 0.917, 0.909, 0.918, 0.914, 0.853, 0.689, 0.668, 0.779, 0.734, and 0.734, all of which are between 0.62 and 0.92.

PCA analysis results. The S1–S18 common peak data were imported into the SIMCA software, the missing value was filled with half of the minimum value, and the component was eliminated if the missing value reached 20%. The PCA approach was used for statistically analyzing the HPLC data matrix (Fig 6). *R. tanguticum* grown in Gannan and Qinghai had a tendency to separate t[2], however this trend was not noticeable.

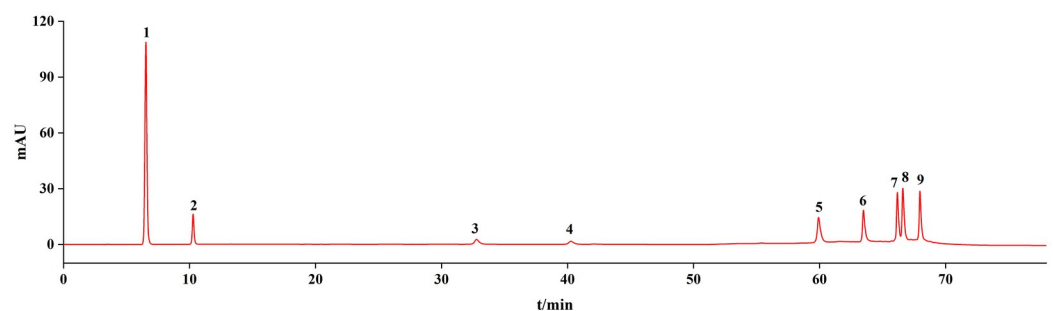


Fig 3. Chromatogram of pharmacopoeia standards. 1: Gallic acid, 2: (+)-catechin, 3: Sennoside B, 4: Sennoside A, 5: Aloe emodin, 6: Rhein, 7: Emodin, 8: Chrysophanol, 9: Emodin methyl ether.

<https://doi.org/10.1371/journal.pone.0278113.g003>

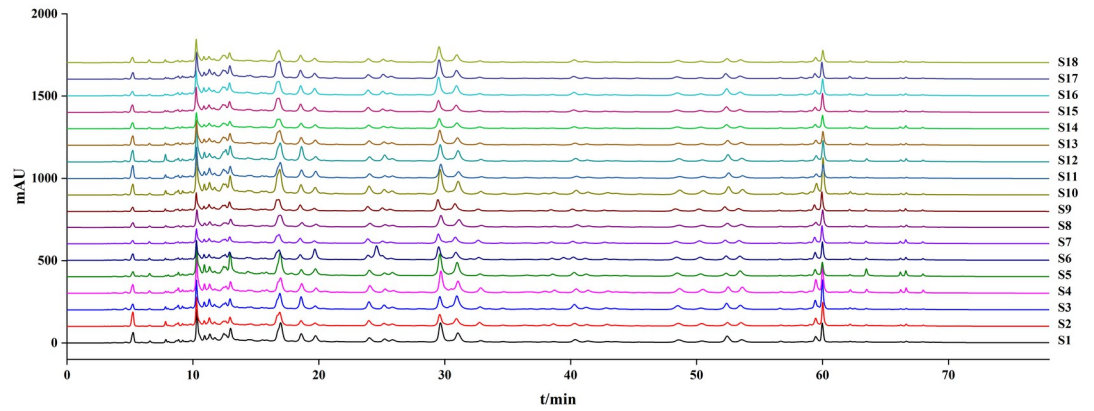


Fig 4. The chromatograms of S1 ~ S18.

<https://doi.org/10.1371/journal.pone.0278113.g004>

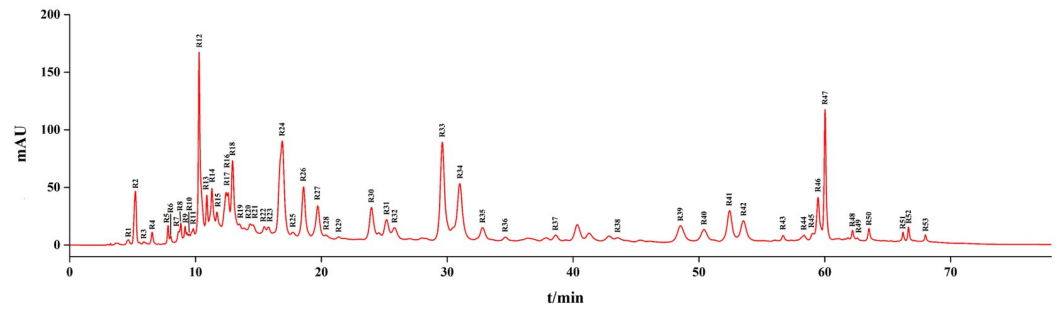


Fig 5. The chromatogram of S1 ~ S18 (common peak mode). R4: Gallic acid, R12: (+)—catechin, R35: Sennoside B, R47: Aloe emodin, R50: Rhein, R51: Emodin, R52: Chrysophanol, R53: Emodin methyl ether.

<https://doi.org/10.1371/journal.pone.0278113.g005>

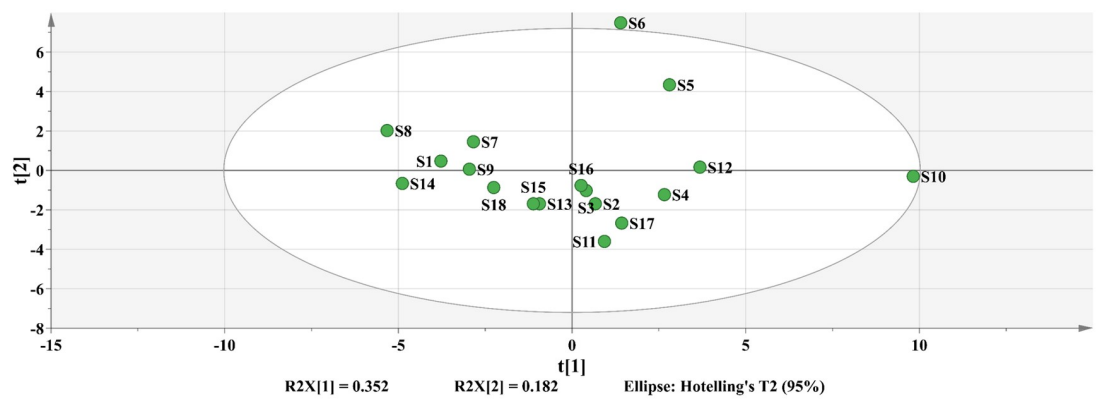


Fig 6. PCA analysis of S1~S18.

<https://doi.org/10.1371/journal.pone.0278113.g006>

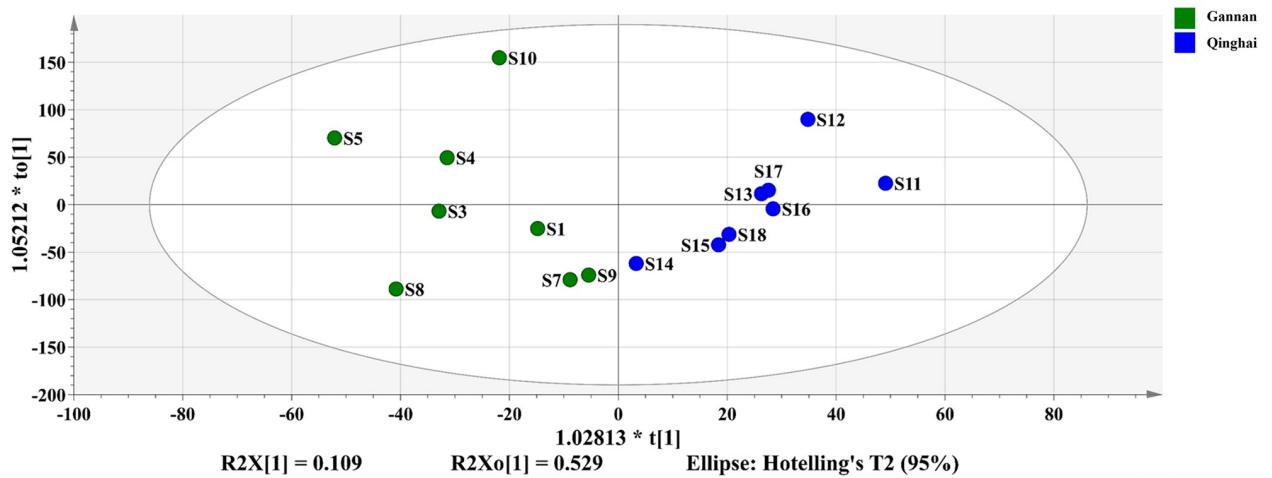


Fig 7. OPLS-DA.

<https://doi.org/10.1371/journal.pone.0278113.g007>

OPLS-DA analysis results. According to the PCA findings, S2 (spring harvest) and S6 (outside the 95 percent confidence interval) were removed from further investigation of the component differences of *R. tanguticum* produced in Gannan and Qinghai. The remaining samples were separated into two groups based on their origin, Gannan and Qinghai. OPLS-DA analysis was performed between the groups, and the OPLS-DA score diagram and S-plot diagram were generated (Figs 7–9). In the OPLS-DA study, $R^2Y = 0.780$ and $Q^2 = 0.550$, suggesting that the two groups were well divided and that the model could predict 55.0% of the results. Permute the OPLS-DA model 200 times (Fig 10), $R^2 = 0.637$, $Q^2 = -0.397$, suggesting that the model is correct.

The larger was the variable importance of projection (VIP) value of the point farther from the origin of the "s" curve in the figure, the greater was the contribution to the grouping. According to the s-plot analysis, coupled with the VIP value (Fig 9). Components with a $VIP \geq 1$ were eliminated, and compounds with differences were found in conjunction with $P < 0.05$. According to these findings, R16, R37, R46, and R47 (Aloe emodin) are the key differentiating components of *Rheum tanguticum* produced in Gannan and Qinghai.

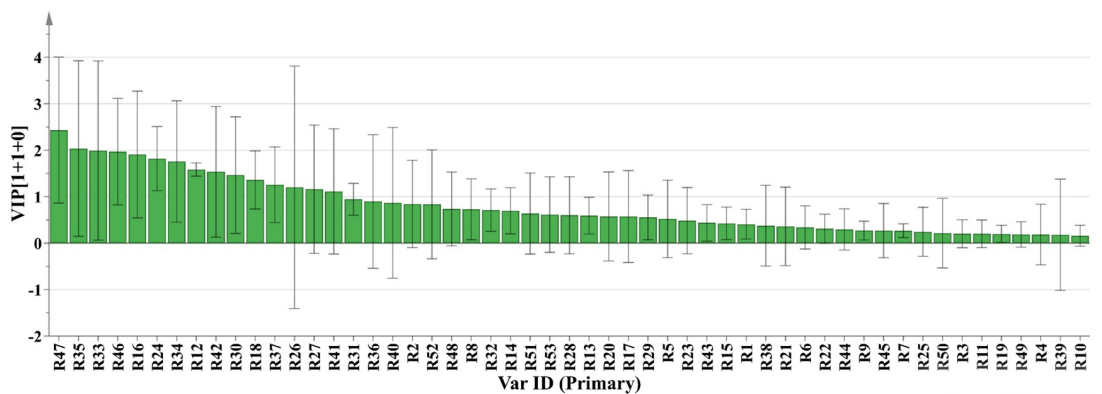


Fig 8. Permutations.

<https://doi.org/10.1371/journal.pone.0278113.g008>

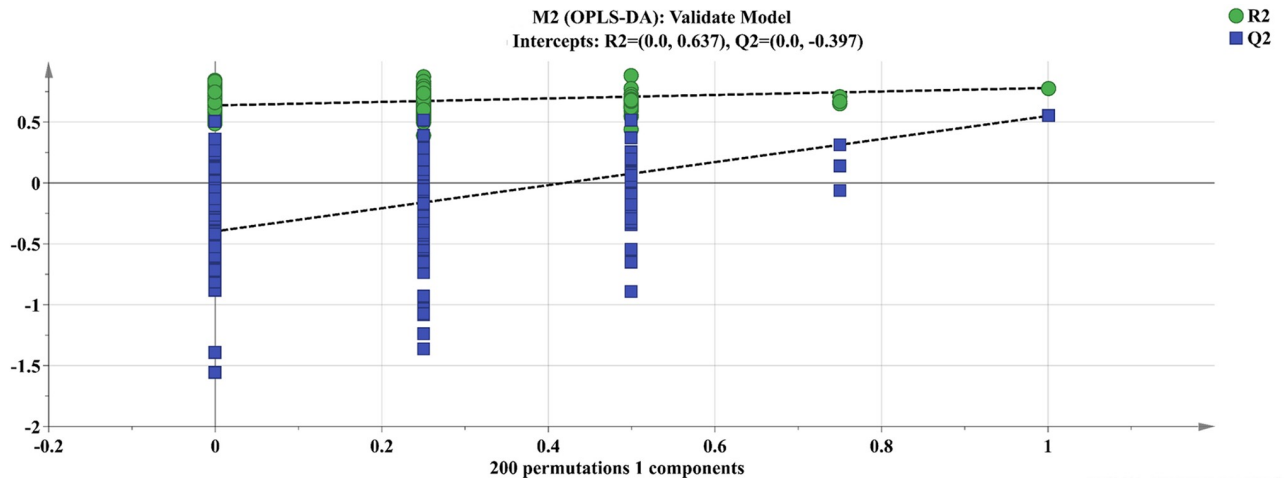


Fig 9. S-Plot.

<https://doi.org/10.1371/journal.pone.0278113.g009>

Influence of longitude, latitude and altitude on composition

Pearson's correlation coefficient was used to examine the relationship between longitude, latitude, altitude, and composition (Table 9). Longitude was significantly positively correlated with R28 and R30 ($P < 0.05$), and a very significantly positively correlated with R35, R36, R37, R46, and R47 ($P < 0.01$). Latitude was significantly negatively correlated with R34, R35, and R40 ($P < 0.05$), and extremely significantly negatively correlated with R28, R30, R36, R37, R46, and R47 ($P < 0.01$). Altitude was significantly positive correlation with R36 and R37 ($P < 0.01$).

Discussion

The fingerprints of *R. tanguticum* are extensively researched; however, the distinctions between *R. tanguticum* from different production locations are still not well investigated. FTIR spectroscopy was used to examine the methanol extract of *R. tanguticum* from various production sites. According to cluster analysis, some discrepancies existed in the FTIR spectra from various manufacturing locations. The double index analysis sequence of the common peak

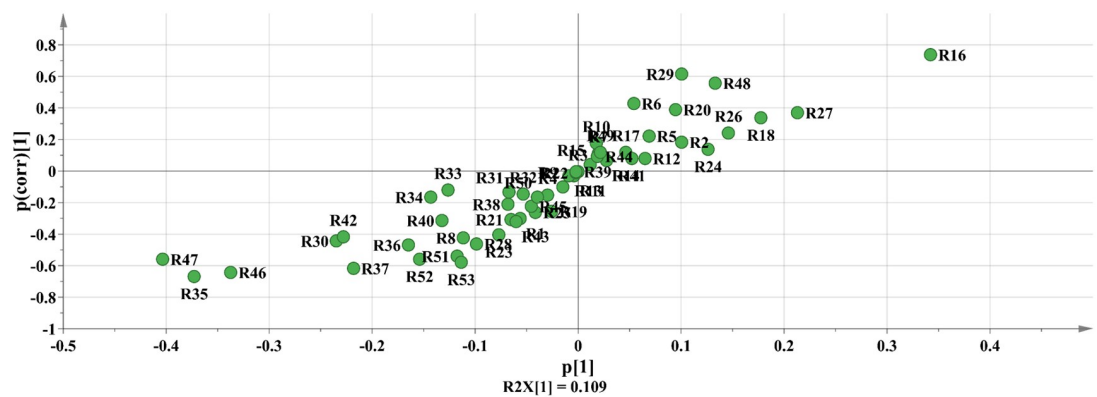


Fig 10. VIP Value.

<https://doi.org/10.1371/journal.pone.0278113.g010>

Table 9. Pearson correlation test table for the influence of longitude, latitude and altitude on composition.

Composition	Longitude		Latitude		Altitude	
	Correlation Coefficient	Significance	Correlation Coefficient	Significance	Correlation Coefficient	Significance
R1	0.291	0.241	-0.213	0.396	-0.063	0.804
R2	0.126	0.618	0.093	0.712	-0.333	0.178
R3	0.483	0.188	-0.345	0.363	0.242	0.531
R4	0.242	0.333	-0.314	0.204	-0.260	0.298
R5	0.109	0.668	-0.026	0.918	-0.311	0.209
R6	-0.061	0.810	0.052	0.837	-0.274	0.272
R7	0.275	0.285	-0.129	0.621	-0.032	0.903
R8	0.401	0.099	-0.342	0.164	0.188	0.455
R9	0.251	0.315	-0.186	0.460	0.140	0.579
R10	-0.115	0.660	0.200	0.443	-0.013	0.961
R11	0.055	0.827	-0.016	0.949	0.097	0.703
R12	0.233	0.353	-0.130	0.606	-0.035	0.891
R13	0.170	0.501	-0.202	0.421	-0.167	0.507
R14	0.229	0.360	-0.081	0.748	0.203	0.419
R15	0.079	0.754	0.081	0.748	0.108	0.671
R16	-0.216	0.389	0.314	0.204	-0.327	0.185
R17	-0.040	0.883	0.096	0.725	-0.102	0.708
R18	-0.011	0.966	0.087	0.732	-0.154	0.541
R19	0.434	0.159	-0.344	0.273	0.112	0.728
R20	0.093	0.732	-0.172	0.524	0.011	0.969
R21	0.416	0.123	-0.265	0.341	0.480	0.070
R22	0.045	0.869	0.036	0.896	-0.193	0.473
R23	0.389	0.111	-0.254	0.309	0.300	0.227
R24	0.135	0.594	-0.017	0.945	-0.046	0.857
R25	0.544	0.055	-0.414	0.160	0.272	0.368
R26	-0.185	0.463	0.174	0.490	-0.146	0.564
R27	-0.126	0.618	0.124	0.624	-0.198	0.431
R28	0.616*	0.025	-0.738**	0.004	0.366	0.218
R29	-0.491	0.217	0.540	0.167	0.123	0.772
R30	0.548*	0.028	-0.649**	0.007	0.341	0.196
R31	0.347	0.296	-0.347	0.296	0.102	0.766
R32	0.382	0.246	-0.382	0.246	0.066	0.847
R33	0.328	0.299	-0.328	0.299	0.213	0.506
R34	0.521	0.056	-0.595*	0.025	0.456	0.101
R35	0.773**	0.002	-0.617*	0.025	0.276	0.362
R36	0.704**	0.003	-0.704**	0.003	0.655**	0.008
R37	0.821**	0.002	-0.821**	0.002	0.749**	0.008
R38	0.574	0.106	-0.495	0.175	0.455	0.218
R39	0.345	0.299	-0.556	0.076	0.374	0.258
R40	0.585	0.059	-0.642*	0.033	0.249	0.460
R41	0.240	0.452	-0.166	0.605	0.122	0.706
R42	0.465	0.175	-0.518	0.125	0.269	0.453
R43	0.403	0.109	-0.458	0.065	0.468	0.058
R44	0.019	0.946	-0.099	0.715	0.226	0.400
R45	0.351	0.264	-0.307	0.332	0.373	0.233
R46	0.652**	0.005	-0.719**	0.001	0.307	0.231

(Continued)

Table 9. (Continued)

Composition	Longitude		Latitude		Altitude	
	Correlation Coefficient	Significance	Correlation Coefficient	Significance	Correlation Coefficient	Significance
R47	0.634**	0.005	-0.616**	0.006	0.407	0.093
R48	-0.354	0.163	0.252	0.329	-0.029	0.911
R49	0.373	0.232	-0.315	0.319	-0.154	0.633
R50	0.105	0.677	-0.097	0.703	0.155	0.538
R51	0.358	0.145	-0.294	0.236	0.145	0.567
R52	0.358	0.145	-0.266	0.286	0.201	0.424
R53	0.258	0.317	-0.188	0.469	0.173	0.507

*, at the level of 0.05 (two tailed), the correlation is significant;

**, At the level of 0.01 (two tailed), the correlation is significant.

<https://doi.org/10.1371/journal.pone.0278113.t009>

and variation peak was further established, which can differentiate various production locations of medicinal materials to some extent. The alcohol extract may reduce the impact of several water-soluble components. To further investigate the relationship between components and production areas, the HPLC fingerprint of *R. tanguticum* was established, and chemical pattern discriminant analysis, such as PCA and OPLS-DA analysis, was introduced into the differential component analysis of *R. tanguticum* from different production areas. Differential components of *R. tanguticum* from Gannan and Qinghai were obtained for their distinction. The three elements of longitude, latitude, and altitude were preliminarily identified by evaluating the sample collection information, and the link between the different components and these three factors was built using multiple linear regression. Regression equations between the nine components and longitude and latitude were effectively established, and the link between longitude and latitude and components was discussed further.

The quality of *R. tanguticum* varied according to the growing environment. In terms of composition, R16 of *R. tanguticum* produced in Gannan was substantially lower than that produced in Qinghai ($P < 0.05$), whereas R37, R46, and R47 were significantly greater ($P < 0.05$). Longitude, latitude, and altitude all impacted the quality of medicinal products because they had an influence on the components. This can guide us in determining the origin of therapeutic ingredients and provides a theoretical basis for planting *R. tanguticum* in various production locations.

The quality of *R. tanguticum* depends on numerous factors, including temperature, humidity, precipitation, illumination time, longitude, latitude, altitude, slope, and soil characteristics. The longitude, latitude, and altitude evaluated in the experiment were merely a subset of the influencing elements, which have limits and cannot fully account for the impact of growth factors on the quality of *R. tanguticum*. Furthermore, human elements are critical for the widespread adoption of artificial farming [40]. Consequently, different growth environments can be included in the scope for investigating further development and utilization of *R. tanguticum*, and ecological factors that promote the accumulation of secondary metabolites can be fully considered to improve the quality of medicinal materials. In conclusion, the results of our study can provide insights in its quality control and aid in establishing a natural medication traceability system.

Conclusions

The different production locations of *R. tanguticum* can be distinguished using FTIR and HPLC. The double index analysis sequence of common and variation peaks may differentiate

distinct production locations of medicinal materials. The composition of *R. tanguticum* components from various sources varied substantially by the result of OPLS-DA. The key differential components of *R. tanguticum* produced in Gannan and Qinghai were discovered to be R16, R37, R46, and R47 (Aloe emodin) ($VIP \geq 1$ and $P < 0.05$). Longitude, latitude, and altitude were all found to impact *R. tanguticum* quality by influencing the accumulation of components. Longitude was significantly positively correlated with R28 and R30 ($P < 0.05$), and a very significantly positively correlated with R35, R36, R37, R46, and R47 ($P < 0.01$). Latitude was significantly negatively correlated with R34, R35, and R40 ($P < 0.05$), and extremely significantly negatively correlated with R28, R30, R36, R37, R46, and R47 ($P < 0.01$). Altitude was significantly positive correlation with R36 and R37 ($P < 0.01$). The findings of this study can be used to plan planting of *R. tanguticum*.

Acknowledgments

We would like to thank Yuwei Gan for his assistance in identifying *R. tanguticum*. Thanks to Gansu University of Chinese Medicine's undergraduate teaching practice center for providing the instruments and locations. We would like to thank Editage (www.editage.cn) for English language editing.

Author Contributions

Data curation: Yafei Guo, Qiang Cao, Junmei Wang.

Formal analysis: Yafei Guo, Qiang Cao.

Funding acquisition: Mei Guo.

Investigation: Yafei Guo, Qiang Cao.

Methodology: Yafei Guo, Qiang Cao.

Project administration: Mei Guo.

Supervision: Mei Guo.

Writing – original draft: Yafei Guo, Qiang Cao.

Writing – review & editing: Yafei Guo, Renbo Kou, Leilei Ye.

References

1. Wang X, Yang R, Feng S, Hou X, Zhang Y, Li Y, et al. Genetic variation in *Rheum palmatum* and *Rheum tanguticum* (Polygonaceae), two medicinally and endemic species in China using ISSR markers. *PLoS One*. 2012; 7(12):e51667. Epub 2013/01/05. <https://doi.org/10.1371/journal.pone.0051667> PMID: 23289054.
2. Gao LL, Guo T, Xu XD, Yang JS. Rapid identification and simultaneous analysis of multiple constituents from *Rheum tanguticum* Maxim. ex Balf. by UPLC/Q-TOF-MS. *Nat Prod Res*. 2017; 31(13):1529–35. Epub 2017/01/24. <https://doi.org/10.1080/14786419.2017.1280491> PMID: 28111967.
3. Keshavarzi Z, Shakeri F, Maghool F, Jamialahmadi T, Johnston TP, Sahebkar A. A Review on the Phytochemistry, Pharmacology, and Therapeutic Effects of *Rheum ribes*. *Adv Exp Med Biol*. 2021; 1328:447–61. Epub 2022/01/05. https://doi.org/10.1007/978-3-030-73234-9_30 PMID: 34981496.
4. Aichner D, Ganzera M. Analysis of anthraquinones in rhubarb (*Rheum palmatum* and *Rheum officinale*) by supercritical fluid chromatography. *Talanta*. 2015; 144:1239–44. Epub 2015/10/11. <https://doi.org/10.1016/j.talanta.2015.08.011> PMID: 26452953.
5. Cao YJ, Pu ZJ, Tang YP, Shen J, Chen YY, Kang A, et al. Advances in bio-active constituents, pharmacology and clinical applications of rhubarb. *Chin Med*. 2017; 28(12):36. Epub 2017/12/28. <https://doi.org/10.1186/s13020-017-0158-5> PMID: 29299052.

6. Hu J, Li P, Zhang T. Rhubarb combined with trypsin inhibitor for severe acute pancreatitis: A systematic review and meta-analysis. *Phytother Res.* 2018; 32(8): 1450–1458. Epub 2018/04/19. Epub 2018 Apr 19. <https://doi.org/10.1002/ptr.6096> PMID: 29672966.
7. Zhang WF, Li ZT, Fang JJ, Wang GB, Yu Y, Liu ZQ, et al. Expression and clinical significance of rhubarb on serum amylase and TNF-alpha of rat model of acute pancreatitis. *J Biol Regul Homeost Agents.* 2017; 31(3): 753–760. Epub 2017/09/06. PMID: 28956428.
8. Zhou Y, Wang L, Huang X, Li H, Xiong Y. Add-on effect of crude rhubarb to somatostatin for acute pancreatitis: A meta-analysis of randomized controlled trials. *J Ethnopharmacol.* 2016; 194(24): 495–505. Epub 2016/09/29. <https://doi.org/10.1016/j.jep.2016.09.053> PMID: 27693773.
9. Guo Y, Li Y, Cao Q, Ye L, Wang J, Guo M. The Function of Natural Polysaccharides in the Treatment of Ulcerative Colitis. *Front Pharmacol.* 2022; 13: 927855. Epub 2022/07/04. <https://doi.org/10.3389/fphar.2022.927855> PMID: 35860025.
10. Hu J, Li P, Zhang T. Rhubarb combined with trypsin inhibitor for severe acute pancreatitis: A systematic review and meta-analysis. *Phytother Res.* 2018; 32(8):1450–8. Epub 2018/04/20. <https://doi.org/10.1002/ptr.6096> PMID: 29672966.
11. Moon MK, Kang DG, Lee JK, Kim JS, Lee HS. Vasodilatory and anti-inflammatory effects of the aqueous extract of rhubarb via a NO-cGMP pathway. *Life Sci.* 2006; 78(14):1550–7. Epub 2005/11/05. <https://doi.org/10.1016/j.lfs.2005.07.028> PMID: 16269157.
12. Neyrinck AM, Etxeberria U, Taminiau B, Daube G, Van Hul M, Everard A, et al. Rhubarb extract prevents hepatic inflammation induced by acute alcohol intake, an effect related to the modulation of the gut microbiota. *Mol Nutr Food Res.* 2017; 61(1). Epub 2016/06/01. <https://doi.org/10.1002/mnfr.201500899> PMID: 26990039.
13. Cui HX, Zhang LS, Luo Y, Yuan K, Huang ZY, Guo Y. A Purified Anthraquinone-Glycoside Preparation From Rhubarb Ameliorates Type 2 Diabetes Mellitus by Modulating the Gut Microbiota and Reducing Inflammation. *Front Microbiol.* 2019; 25(10): 1423. Epub 2019/06/25. <https://doi.org/10.3389/fmicb.2019.01423> PMID: 31293553.
14. Stompor-Goracy M. The Health Benefits of Emodin, a Natural Anthraquinone Derived from Rhubarb-A Summary Update. *Int J Mol Sci.* 2021; 22(17). Epub 2021/09/11. <https://doi.org/10.3390/ijms22179522> PMID: 34502424.
15. Usui TIY, Tagami T, Matsuda K, Moriyama K, Yamada K, Kuzuya H, Kohno S, Shimatsu A. <The phytochemical lindleyin isolate Source J Endocrinol SO 2002 Nov 175 2 289 96.PDF>. *J Endocrinol.* 2002; 175(2):289–96. <https://doi.org/10.1677/joe.0.1750289> PMID: 12429027
16. Liang Z, Ren C. Emodin attenuates apoptosis and inflammation induced by LPS through up-regulating lncRNA TUG1 in murine chondrogenic ATDC5 cells. *Biomed Pharmacother.* 2018; 103:897–902. Epub 2018/05/02. <https://doi.org/10.1016/j.biopha.2018.04.085> PMID: 29710506.
17. Wen Q M J, Lau N., Zhang C., Ye P., Du S., Mei L., Weng H., Xu Q., Liu X., Chen D., Zhang F., Li C., Li H. Rhein attenuates lipopolysaccharide-primed inflammation through NF-kappaB inhibition in RAW264.7 cells: targeting the PPAR-gamma signal pathway. *Can J Physiol Pharmacol.* 2020; 98(6):357–65. <https://doi.org/10.1139/cjpp-2019-0389> PMID: 31846359
18. Zhu T, Zhang W, Feng SJ, Yu HP. Emodin suppresses LPS-induced inflammation in RAW264.7 cells through a PPARgamma-dependent pathway. *Int Immunopharmacol.* 2016; 34:16–24. Epub 2016/02/26. <https://doi.org/10.1016/j.intimp.2016.02.014> PMID: 26910236.
19. Su S, Wu J, Gao Y, Luo Y, Yang D, Wang P. The pharmacological properties of chrysophanol, the recent advances. *Biomed Pharmacother.* 2020; 125:110002. Epub 2020/02/18. <https://doi.org/10.1016/j.biopha.2020.110002> PMID: 32066044.
20. Qu J, Zhang T, Liu J, Su Y, Wang H. Considerations for the Quality Control of Newly Registered Traditional Chinese Medicine in China: A Review. *J AOAC Int.* 2019; 102(3):689–694. Epub 2018/11/02. <https://doi.org/10.5740/jaoacint.18-0301> PMID: 30381092.
21. Shrimali D, Shanmugam MK, Kumar AP, Zhang J, Tan BK, Ahn KS, et al. Targeted abrogation of diverse signal transduction cascades by emodin for the treatment of inflammatory disorders and cancer. *Cancer Lett.* 2013; 341(2): 139–49. Epub 2013/08/17. <https://doi.org/10.1016/j.canlet.2013.08.023> PMID: 23962559.
22. Ge H, Tang H, Liang Y, Wu J, Yang Q, Zeng L, et al. Rhein attenuates inflammation through inhibition of NF-kB and NALP3 inflammasome in vivo and in vitro. *Drug Des Devel Ther.* 2017; 11: 1663–1671. Epub 2017/06/06. <https://doi.org/10.2147/DDDT.S133069> PMID: 28652704.
23. Ye B, Chen X, Dai S, Han J, Liang X, Lin S, et al. Emodin alleviates myocardial ischemia/reperfusion injury by inhibiting gasdermin D-mediated pyroptosis in cardiomyocytes. *Drug Des Devel Ther.* 2019; 25(13): 975–990. Epub 2019/03/25. <https://doi.org/10.2147/DDDT.S195412> PMID: 30988600.

24. Zhu T, Zhang W, Feng SJ, Yu HP. Emodin suppresses LPS-induced inflammation in RAW264.7 cells through a PPAR γ -dependent pathway. *Int Immunopharmacol.* 2016; 34: 16–24. Epub 2016/02/22. <https://doi.org/10.1016/j.intimp.2016.02.014> PMID: 26910236.
25. Zhou Y, Gao C, Vong CT, Tao H, Li H, Wang S, et al. Rhein regulates redox-mediated activation of NLRP3 inflammasomes in intestinal inflammation through macrophage-activated crosstalk. *Br J Pharmacol.* 2022; 179(9): 1978–1997. Epub 2022/01/06. <https://doi.org/10.1111/bph.15773> PMID: 34882785.
26. Liu M, Wang L, Wu X, Gao K, Wang F, Cui J, et al. Rhein protects 5/6 nephrectomized rat against renal injury by reducing inflammation via NF- κ B signaling. *Int Urol Nephrol.* 2021; 53(7): 1473–1482. Epub 2021/03/25. <https://doi.org/10.1007/s11255-020-02739-w> PMID: 33763781.
27. Zhuang S, Zhong J, Zhou Q, Zhong Y, Liu P, Liu Z. Rhein protects against barrier disruption and inhibits inflammation in intestinal epithelial cells. *Int Immunopharmacol.* 2019; 71: 321–327. Epub 2019/04/02. <https://doi.org/10.1016/j.intimp.2019.03.030> PMID: 30952096.
28. Sun M, Wu H, He M, Jia Y, Wang L, Liu T, et al. Integrated assessment of medicinal rhubarb by combination of delayed luminescence and HPLC fingerprint with emphasized on bioactivities based quality control. *Chin Med.* 2020; 15:72. Epub 2020/07/21. <https://doi.org/10.1186/s13020-020-00352-8> PMID: 32684945.
29. Wang Y H X, Liang QH, Fan R, Qin F, Guo Y, Yan KP, Liu W, Luo JK, Li YH, Mao XL, Liu ZQ, Zhou HH. A strategy for detecting absorbed bioactive compounds for quality control in the water extract of rhubarb by ultra performance liquid chromatography with photodiode array detector. *Chin J Integr Med.* 2012; 18(9):690–8. <https://doi.org/10.1007/s11655-012-1053-7> PMID: 22936323
30. Zhang L, Liu H, Qin L, Zhang Z, Wang Q, Zhang Q, et al. Global chemical profiling based quality evaluation approach of rhubarb using ultra performance liquid chromatography with tandem quadrupole time-of-flight mass spectrometry. *J Sep Sci.* 2015; 38(3):511–22. Epub 2014/12/06. <https://doi.org/10.1002/jssc.201400971> PMID: 25476582.
31. Wang J, Li H, Jin C, Qu Y, Xiao X. Development and validation of a UPLC method for quality control of rhubarb-based medicine: fast simultaneous determination of five anthraquinone derivatives. *J Pharm Biomed Anal.* 2008; 47(4–5):765–70. Epub 2008/04/29. <https://doi.org/10.1016/j.jpba.2008.03.011> PMID: 18440751.
32. Klein-Junior LC, de Souza MR, Viaene J, Bresolin TMB, de Gasper AL, Henriques AT, et al. Quality Control of Herbal Medicines: From Traditional Techniques to State-of-the-art Approaches. *Planta Med.* 2021; 87(12–13):964–88. Epub 2021/08/20. <https://doi.org/10.1055/a-1529-8339> PMID: 34412146.
33. Song X-Y, Li Y-D, Shi Y-P, Jin L, Chen J. Quality control of traditional Chinese medicines: a review. *Chinese Journal of Natural Medicines.* 2013; 11(6):596–607. [https://doi.org/10.1016/S1875-5364\(13\)60069-2](https://doi.org/10.1016/S1875-5364(13)60069-2) PMID: 24345500
34. Jiang H, Zhang Y, Liu Z, Wang X, He J, Jin H. Advanced applications of mass spectrometry imaging technology in quality control and safety assessments of traditional Chinese medicines. *Journal of Ethnopharmacology.* 2022; 284. <https://doi.org/10.1016/j.jep.2021.114760> PMID: 34678417
35. Li Y, Geng L, Liu Y, Chen M, Mu Q, Zhang X, et al. Identification of three *Daphne* species by DNA barcoding and HPLC fingerprint analysis. *PLoS One.* 2018; 13(8):e0201711. Epub 2018/08/03. <https://doi.org/10.1371/journal.pone.0201711> PMID: 30071090 Pass (Qinhuangdao 066200, China) which provided great financial support. The funder did not have any additional role in the study design, data collection and analysis, decision to publish, or preparation of the manuscript. This commercial affiliation does not alter our adherence to all PLOS ONE policies on sharing data and materials.
36. Javier-Astete R, Jimenez-Davalos J, Zolla G. Determination of hemicellulose, cellulose, holocellulose and lignin content using FTIR in *Calycophyllum spruceanum* (Benth.) K. Schum. and *Guazuma crinita* Lam. *PLoS One.* 2021; 16(10):e0256559. Epub 2021/10/28. <https://doi.org/10.1371/journal.pone.0256559> PMID: 34705842.
37. Cao Z, Wang Z, Shang Z, Zhao J. Classification and identification of *Rhodobryum roseum* Limpr. and its adulterants based on fourier-transform infrared spectroscopy (FTIR) and chemometrics. *PLoS One.* 2017; 12(2):e0172359. Epub 2017/02/17. <https://doi.org/10.1371/journal.pone.0172359> PMID: 28207900.
38. Ohta T, Uto T, Tanaka H. Effective methods for increasing coumestrol in soybean sprouts. *PLoS One.* 2021; 16(11):e0260147. Epub 2021/11/19. <https://doi.org/10.1371/journal.pone.0260147> PMID: 34793574.
39. Zhou Y, Li W, Han LF, Song XB, Li PF, Wang R, et al. Identification of Chinese Traditional Medicine *Cistanches Herba* from Different Places by HPLC-ESI-MS and FTIR Methods. *Guang Pu Xue Yu Guang Pu Fen Xi.* 2015; 35(4):1056–61. PMID: 26197602.
40. Xiong F, Nie X, Zhao X, Yang L, Zhou G. Effects of different nitrogen fertilizer levels on growth and active compounds of rhubarb from Qinghai plateau. *J Sci Food Agric.* 2019; 99(6):2874–82. Epub 2018/11/22. <https://doi.org/10.1002/jsfa.9500> PMID: 30460686.